Title

Electrophysiology and metabolism of caveolin-3-overexpressing mice

Journal

Basic Research in Cardiology, 111(3)

ISSN

0300-8428

Authors

Schilling, Jan M

Horikawa, Yousuke T

Zemljic-Harpf, Alice E

et al.

Publication Date

2016-05-01

DOI

10.1007/s00395-016-0542-9

Peer reviewed

HHS Public Access

Author manuscript

Basic Res Cardiol. Author manuscript; available in PMC 2017 May 01.

Published in final edited form as:

Basic Res Cardiol. 2016 May ; 111(3): 28. doi:10.1007/s00395-016-0542-9.

Electrophysiology and metabolism of caveolin-3 overexpressing mice

Jan M. Schilling[*,1,2], **Yousuke T. Horikawa**[*,3,6], **Alice E. Zemljic-Harpf**[1,2], **Kevin P. Vincent**[4], **Leonid Tyan**[7], **Judith K. Yu**[2], **Andrew D. McCulloch**[4,5], **Ravi C. Balijepalli**[7], **Hemal H. Patel**[1,2], and **David M. Roth**[1,2]

[1]Veterans Affairs San Diego Healthcare System, San Diego, CA, USA

[2]Department of Anesthesiology, University of California San Diego, La Jolla, CA, USA

[3]Department of Pediatrics, University of California San Diego, La Jolla, CA, USA

[4]Department of Bioengineering, University of California San Diego, La Jolla, CA, USA

[5]Department of Medicine, University of California San Diego, La Jolla, CA, USA

[6]Department of Pediatrics, Sharp Rees-Stealy Medical Group, San Diego, CA, USA

[7]Department of Medicine, Cellular and Molecular Arrhythmia Research Program, University of Wisconsin, Madison, Wisconsin, USA

Abstract

Caveolin-3 (Cav-3) plays a critical role in organizing signaling molecules and ion channels involved in cardiac conduction and metabolism. Mutations in Cav-3 are implicated in cardiac conduction abnormalities and myopathies. Additionally, cardiac specific overexpression of Cav-3 (Cav-3 OE) is protective against ischemic and hypertensive injury suggesting a potential role for Cav-3 in basal cardiac electrophysiology and metabolism involved in stress adaptation. We hypothesized that overexpression of Cav-3 may alter baseline cardiac conduction and metabolism. We examined: 1) ECG telemetry recordings at baseline and during pharmacological interventions, 2) ion channels involved in cardiac conduction with immunoblotting and computational modeling, and 3) baseline metabolism in Cav-3 OE and transgene negative littermate control mice. Cav-3 OE mice had decreased heart rates, prolonged PR intervals, and shortened QTc intervals with no difference in activity compared to control mice. Dobutamine or propranolol did not cause significant changes between experimental groups in maximal (dobutamine) or minimal (propranolol) heart rate. Cav-3 OE mice had an overall lower chronotropic response to atropine. Expression of $K_v1.4$ and $K_v4.3$ channels, $Na_v1.5$ channels and connexin 43 were increased in Cav-3 OE mice. A computational model integrating the immunoblotting results indicated shortened action potential duration in Cav-3 OE mice linking the change in channel expression to the observed electrophysiology phenotype. Metabolic profiling showed no gross differences in VO_2, VCO_2, respiratory exchange ratio, and heat generation, feeding or drinking. In conclusion,

Corresponding Author: David M. Roth, PhD, MD, University of California, San Diego, VA Medical Center, San Diego (125), 3350 La Jolla Village Drive, San Diego, CA 92161-5085, Phone: (858) 552-8585, FAX (858) 534-0104, droth@ucsd.edu.

*Joint first authors

The authors have no additional financial disclosures.

Cav-3 OE mice have changes in ECG intervals, heart rates, and cardiac ion channel expression. These findings give novel mechanistic insights into previously reported Cav-3 dependent cardioprotection.

Keywords

caveolae; caveolin-3; cardiac conduction; heart rate; K_v channels

Introduction

Caveolae are small “flask like” invaginations of the sarcolemmal membrane discovered over six decades ago [37, 63]. Recent work has identified caveolae as signaling epicenters made up of essential scaffolding proteins called caveolins. Caveolae and caveolins are necessary for the precise temporal and spatial localization and organization of cellular signaling molecules [22, 38] involved in cardiac protection [21, 46, 55, 57, 58] and cardiac remodeling [20]. There are three distinct caveolin (Cav) isoforms including Cav-1 and Cav-2, which are ubiquitous in all cell types and Cav-3, which is found predominantly in skeletal and cardiac myocytes [11, 41, 52]. Cav-3, via its scaffolding domain has been shown to interact with numerous signaling molecules including G-protein coupled receptors (GPCRs), ion channels and receptor tyrosine kinases [22, 38, 53]. Mice with cardiac specific overexpression of caveolin-3 (Cav-3 OE) demonstrate tolerance to myocardial ischemia and left ventricular pressure overload suggesting stress adaptation of the heart [20, 56].

Cav-3 plays an integral role in organizing signaling molecules that are essential for the generation of heart rate, rhythm and cardiac chronotropy [10, 29, 59, 66]. Cav-3 mutations have been implicated in cardiac arrhythmias, particularly prolonged QT syndrome, given their association with adrenergic receptors and ion channels. Furthermore, specific chronotropic ion channels have been localized within caveolae including SCN5A-encoded voltage-gated Na^+ channels [65], voltage-dependent K^+ channel [2], sodium calcium exchangers [7, 8], and L-Type Ca^{2+} channels [3, 28].

Despite these provocative findings regarding Cav-3 expression and cardiac conduction there are no data regarding the effect of Cav-3 overexpression in the heart on basic electrophysiology and metabolism. In the current study we describe baseline cardiac conduction and metabolism in Cav-3 OE mice as a means to add mechanistic insight into the alterations in stress adaption previously observed in Cav-3 OE mice.

Materials and Methods

Animals

All mice were treated in compliance with the *Guide for the Care and Use of Laboratory Animals* (National Academy of Science) and protocols were approved by the VA San Diego Healthcare System Institutional Animal Care and Use Committee. Animals were kept on a 12-hr light-dark cycle (with light on from 6:00h–18:00h) in a temperature-controlled room with *ad libitum* access to food and water. Transgenic mice were generated in our laboratory using the α-myosin heavy chain promoter to produce cardiac myocyte-specific

overexpression of Cav-3 (Cav-3 OE**)** in a C57BL/6 background. Full-length Cav-3 cDNA (455 bp) was cloned into a vector containing the α-myosin heavy chain promoter and was used for microinjection by the UCSD Transgenic Core. Cav-3 OE mice have a ~1.8-fold increase in caveolin-3 protein in whole heart homogenates [55]. Transgene negative littermates were used as control mice. All experiments were performed on male mice.

Telemetry

4-5 month old male Cav-3 OE (*N* = 7/group) and control mice (*N* = 8/group) were anesthetized with 1.4% isoflurane. A small peritoneal incision was made and the transmitter (ETA-F10, Data Sciences International (DSI), Inc, St. Paul, MN) was inserted into the peritoneal cavity and the leads were secured in the right thorax and lower abdominal regions per manufactures protocol. Continuous signals were transmitted wirelessly to the receivers located below the cage. Animals were given analgesia (buprenorphine) and allowed to recover for 72 hours. Mice were then acclimated for 10 days without analgesia. All mice were housed in ventilated cages with *ad libitum* food and water. Light and dark cycles were maintained using automatic timers. Continuous telemetry recordings were monitored for 72 hours using Dataquest ART software (Data Sciences International, Inc., St. Paul, MN) and analyzed with the programs default mouse parameters. QTc was measured using previously published derived equations for conscious mice, QTc=QT/SQRT(RR/100) [32, 68].

Pharmacological Studies

Heart rate response to β-adrenergic stimulation (dobutamine, 4mg/kg), parasympathetic blockade (atropine, 1mg/kg), β-adrenergic blockade (propranolol, 1mg/kg) and autonomic blockade (atropine and propranolol) were obtained. Intra-peritoneal dobutamine was injected and heart rate was averaged over 60 seconds intervals and monitored for 60 minutes. Mice were then allowed to rest 6 hours before being given intra-peritoneal atropine and then heart rate was monitored for 120 minutes with 5 minute intervals. The following day, intra-peritoneal propranolol was injected and heart rate recorded for 5 hours with 15 minute intervals. After six hours, a second injection of propranolol and atropine was given and heart rate was recorded for an additional 120 minutes with 5 minute intervals.

Immunoblotting

Immunoblotting was performed on adult mouse ventricular homogenates prepared from either control or Cav-3 OE mice (*N* = 5 - 7/group). Homogenates were solubilized using ice-cold 11 mmoles/L Tris-HCL pH 7.4, 1.1 mmoles/L EDTA 0.2% SDS, 11% glycerol and protease inhibitors (2 mM phenylmethylsulfonyl fluoride, 12 μg/ml aprotinin, 1 mM benzamidine, 10 μM leupeptin, 5 μM pepstatin A). The lysate was centrifuged at 5,000 g for 10 min to remove insoluble debris. Protein content was estimated in the soluble supernatant and equal amount of each sample was analyzed by SDS/PAGE (4–15% gradient gels, Bio-Rad) and western blot by probing with antibodies to Cav-3, connexin 43 (Cx43) and GAPDH (Millipore), $K_v1.4$, $K_v4.2$ and $K_v4.3$ antibodies (NeuroMab, UC Davis, CA), $Ca_v1.2$ antibody (Alomone labs, Jerusalem, Israel) and $Na_v1.5$ antibody (Millipore Corporation). Protein signals for Cav-3 and channel subunits were quantified by normalizing signal to GAPDH.

Computational Modeling

A recently published murine ventricular action potential model [33] was used to investigate the observed changes in ion channel expression in the Cav-3 OE mice. This computational model consists of a system of 158 ordinary differential equations describing the myocyte ion channels and Ca^{2+} handling as well as PKA and CaMKII signaling networks. The model source code was obtained from the author's website (https://somapp.ucdmc.ucdavis.edu/Pharmacology/bers/) [33], and all simulations were executed using the ode15s algorithm in MATLAB (The MathWorks, Inc., Natick, MA, USA). In the absence of functional ion channel data, previous studies have meaningfully incorporated differences in ion channel transcript levels into an action potential model by scaling the whole-cell ion channel conductance based on relative differences [6, 9]. Similarly, we created a Cav-3 OE version of the action potential model by scaling the ion channel conductance by statistically significant changes in ion channel protein expression measured by western blot. Action potential duration (APD) was measured with respect to the control repolarization levels so that changes in action potential amplitude alone would not alter APD results.

CLAMS Metabolic Cage

Metabolic studies were performed at the UCSD Phenotyping Core facility. In brief, animals were placed in temperature and light controlled CLAMS metabolic cages (Columbus Instruments, Columbus, OH) and oxygen uptake, carbon dioxide output, respiratory exchange ratio (RER), feeding, and drinking were recorded continuously for 2.5 days.

Statistics

Investigators were blinded to the genetic background of mice in all study protocols. Statistical analysis was performed with GraphPad Prism Software v6.0 (La Jolla, CA, USA). All values are presented as mean ± standard deviation [*M (SD)*]. 2-Way or 2-Way repeated measure (RM) ANOVA followed by post-hoc Tukey's correction for multiple comparisons and unpaired Student's *t*-test were utilized. An α-level of $p < 0.05$ for all statistical tests was used.

Results

Cav-3 OE and control mice show similar activity and body temperature during telemetry recording

Cav-3 OE and control mice ($N = 7$ - 8/group) were investigated during telemetry recording and total activity (arbitrary units) was measured. Cav-3 OE mice showed similar activity to control mice over a two and a half day period (**Figure 1A**). In detail, we found a main effect of time ($F(9,117) = 29.57$, $p < 0.001$), with both strains displaying less activity during the light cycle (6:00h – 18:00h), with no main effect of strain ($F(1,13) = 0.34$, $p = 0.570$), or interaction between time and strain ($F(9,117) = 0.50$, $p = 0.872$). In addition, body temperature (°C) was measured continuously. We found a main effect of time ($F(9,117) = 119.4$, $p < 0.001$), with both strains displaying a lower body temperature during the light cycle (6:00h – 18:00h) (**Figure 1B**). No main effect of strain ($F(1,13) = 0.03$, $p = 0.864$) or time and strain interaction was observed ($F(9,117) = 0.37$, $p = 0.949$).

Cav-3 OE mice have lower 24hr heart rates and show higher heart rate fluctuation

Continuous ECG recording in conscious mice (DSI) showed physiological heart rates in control and Cav-3 OE mice; however, heart rates from Cav-3 OE mice changed significantly over time compared to control mice. Control mice ranged from 513 to 555 beats per minute (bpm), whereas Cav-3 OE mice ranged from 468 to 580 bpm during minimal and maximal amounts of activity (**Figure 1C**) with significantly lower resting heart rates. In detail, we found a main effect of time ($F(9,117) = 10.73$, $p < 0.001$), with both strains displaying a lower heart rate during the light cycle (6:00h – 18:00h). No main effect of strain ($F(1,13) = 2.23$, $p = 0.16$) was observed. We furthermore found a significant interaction between time and strain ($F(9,117) = 2.98$, $p = 0.003$), with Cav-3 OE mice showing a higher fluctuation of heart rate with overall lower heart rates recorded. However, the difference between strains was observed more clearly when heart rates were averaged over a 24hr time frame (**Figure 2A**); Cav-3 OE mice ($M = 509.40$ bpm, $SD = 20.56$) had a significant lower heart rate compared to control mice ($M = 535.1$ bpm, $SD = 23.28$; $t(13) = 2.25$, $p = 0.04$).

Cav-3 OE mice have prolonged PR intervals as well as shortened QT intervals

ECG data from Cav-3 OE and control mice ($N = 7$ - 8/group) were analyzed for a 24-hour period. Cav-3 OE mice ($M = 38.51$ msec., $SD = 2.04$) had significantly longer PR interval times compared to control mice (**Figure 2B**; $M = 35.09$ msec., $SD = 1.10$; $t(13) = 4.12$, $p = 0.001$). No significant difference was observed in the QRS interval times when Cav-3 OE mice ($M = 12.97$ msec., $SD = 0.63$) were compared to control mice (**Figure 2C**; $M = 13.10$ msec., $SD = 0.63$; $t(13) = 0.40$, $p = 0.70$). Furthermore, Cav-3 OE mice ($M = 46.82$ msec., $SD = 3.45$) had significantly shorter QTc interval times compared to control mice (**Figure 2D**; $M = 53.95$ msec., $SD = 4.15$; $t(13) = 3.59$, $p = 0.003$).

Cav-3 OE mice have altered heart rate responses to cardiac pharmacological agents when compared to control mice

Conscious Cav-3 OE and control mice ($N = 8$/group) were injected with various inotropic and chronotropic agents and heart rate was recorded (DSI). Analysis was performed for the time period after the injection. Both, Cav-3 OE and control mice exhibited increased chronotropy (~200 bpm) with injection of dobutamine, a known sympathomimetic drug used to stimulate b_1 adrenergic receptors (**Figure 3A**). Interestingly, Cav-3 OE mice recovered nearly 10 minutes sooner than control mice to baseline heart rate. We found a main effect of time ($F(41,533) = 23.66$, $p < 0.001$) with both strains displaying altered heart rates over time. The main effect of strain ($F(1,13) = 4.44$, $p = 0.06$) and interaction between time and strain ($F(41,533) = 0.71$, $p = 0.913$) were not significant. Atropine, a competitive antagonist of the muscarinic acetylcholine receptors, increased heart rate similarly in Cav-3 OE and control mice. However, Cav-3 OE mice had overall lower heart rates in response to atropine compared to control mice (**Figure 3B**). We found a significant main effect of strain ($F(1,13) = 5.30$, $p = 0.039$). No significance of time ($F(21,273) = 1.45$, $p = 0.10$) or interaction between time and strain ($F(21,273) = 0.49$, $p = 0.97$) was observed. Propranolol, a non-selective beta-blocker (**Figure 3C**) caused a maximal reduction in heart rate at ~75 minutes in both groups, but Cav-3 OE mice had sustained lower heart rates for nearly 2 additional hours whereas heart rate in control mice recovered much sooner. We found a main effect of

time ($F(18,234) = 5.56$, $p < 0.001$). We found no significance of strain ($F(1,13) = 4.16$, $p = 0.06$) or interaction between time and strain ($F(18,234) = 0.93$, $p = 0.54$). When both propranolol and atropine were injected, lower heart rates were noted in both groups (**Figure 3D**). However, no significant difference between groups was observed. For these data we found a main effect of time ($F(21,273) = 10.59$, $p < 0.001$) but no significant main effect of strain ($F(1,13) = 1.10$, $p = 0.31$) or interaction between time and strain ($F(21,273) = 0.62$, $p = 0.91$) was observed.

Cav-3 OE mice show increased $K_v1.4$ and $K_v4.3$ potassium channels, $Na_v1.5$ sodium channels and Cx43 expression

As changes in conduction, rate, and rhythm may be linked to changes in ion channel expression, we determined the expression of the major ion channels involved in the cardiac action potential in left ventricles by immunoblot analysis. As shown in **Figure 4**, protein expression of $K_v1.4$ (**Figure 4A**; $N = 5$/group; Cav-3 OE $M = 2.76$, $SD = 0.85$ versus control $M = 1.41$, $SD = 0.67$; $t(8) = 2.78$, $p = 0.02$) and $K_v4.3$ (**Figure 4C**; $N = 5$/group; Cav-3 OE $M = 1.71$, $SD = 0.56$ versus control $M = 0.79$, $SD = 0.33$; $t(8) = 3.18$, $p = 0.01$) was significantly increased in the Cav-3 OE mice compared to control mice, respectively. However, the protein expression of the $K_v4.2$ (**Figure 4B**; $N = 5$/group; Cav-3 OE $M = 1.71$, $SD = 1.58$ versus control $M = 1.59$, $SD = 0.33$; $t(8) = 0.16$, $p = 0.87$), and $Ca_v1.2$ was unchanged between groups (**Figure 4D**; $N = 5$ - 6/group; Cav-3 OE $M = 1.35$, $SD = 0.39$ versus control $M = 0.98$, $SD = 0.32$; $t(9) = 1.72$, $p = 0.12$). Additionally $Na_v1.5$ protein expression (**Figure 4E**; $N = 5$ - 6/group; Cav-3 OE $M = 1.31$, $SD = 0.26$ versus control $M = 0.76$, $SD = 0.48$; $t(9) = 2.41$, $p = 0.04$) and Cx43 expression (**Figure 4F**; $N = 5$ - 6/group; Cav-3 OE $M = 1.28$, $SD = 0.37$ versus control $M = 0.85$, $SD = 0.24$; $t(9) = 2.21$, $p = 0.05$) were significantly increased in Cav-3 OE mice. We performed a confirmatory immunoblot to show that Cav-3 was significantly increased in Cav-3 OE mice (**Figure 4G**; $N = 5$ - 7/group; Cav-3 OE $M = 1.31$, $SD = 0.34$ versus control $M = 0.70$, $SD = 0.42$; $t(10) = 2.78$, $p = 0.02$).

A computation model of ventricular myocytes from Cav-3 OE mice predicted shortened action potential duration

To better understand the effects of altered ion channel expression on the observed electrophysiology phenotype, significant changes in protein expression from **Figure 4** were incorporated into a computation model of a mouse ventricular myocyte action potential. The conductance of the fast component of the transient outward potassium current ($G_{to,f}$), carried by the $K_v4.3$ channel protein, was increased 2.2-fold from 0.44 mS/μF to 0.97 mS/μF, and the conductance of the fast sodium channel (G_{Na}), carried by the $Na_v1.5$ channel protein, was increased 1.7-fold from 10 mS/μF to 17 mS/μF. The slow component of the transient outward potassium current ($I_{to,s}$), carried by the $K_v1.4$ channel protein, was not included in the original model [33] as its expression is typically limited to septal myocytes in the mouse [62].

The resulting Cav-3 action potential model has shortened action potential duration (APD) compared to the control model (**Figure 5A**). The maximum decrease in APD occurred at 50% repolarization (APD_{50}; 55% reduction at 6Hz pacing) with a substantial decrease still

present at 90% repolarization (APD_{90}; 12% at 6 Hz pacing) (**Figure 5B**). This change in APD is consistent across a range of heart rates (**Figure 5C**). Since the largest suppression in APD occurred in the voltage range important for calcium influx, intracellular calcium transients (CaT) were also evaluated in the model. There was a slight reduction in CaT amplitude at 1 Hz pacing (15%) that decreased near physiological rates (9% at 6 Hz pacing) (**Figure 5D**). The relative contributions of each conductance change were dissected by implementing them independently. The increased $G_{to,f}$ was wholly responsible for the decrease in action potential duration (**Figure 5E**). Increasing $G_{to,f}$ and G_{Na} individually had opposing effects on CaT amplitude resulting in the minimal resultant change in the Cav-3 OE model (**Figure 5F**).

Cav-3 OE mice have similar metabolic profiles

In addition to the telemetry studies, we also assessed metabolic parameters using CLAMS metabolic cages. Cav-3 OE and control mice were assessed for two and a half days in CLAMS metabolic cages ($N = 8$/group). Furthermore, while time had a significant effect on all parameters with lower values during the light cycle, we found no statistically significant differences between strains in the weight before, after, weight change, VO_2 (ml/kg/hr), VCO_2 (ml/kg/hr), respiratory exchange ratio (RER), heat (kcal/hr) generation, accumulated feeding (grams), and accumulated drinking (ml). Details and statistical analysis can be found in **Table 1**.

Discussion

Cav-3 has been implicated in playing a role in cardiac rhythm and chronotropy [5, 10, 29, 59, 66] and stress adaptation [20, 55]; however, the effects of cardiac overexpression of Cav-3 on baseline cardiac conduction and metabolism have never been investigated. We have shown for the first time that cardiac specific overexpression of Cav-3 results in significant lower heart rates at rest, prolonged PR interval, shortened QTc intervals and alterations in ion channel expression, while baseline whole organism metabolism remains unchanged.

The normal healthy heart relies on efficient electrical conduction via the sinoatrial node, the atrioventricular node, and the Purkinjie fibers in order to optimize cardiac contraction [14]. The rate at which the heart contracts is modified by various intrinsic and extrinsic signaling mechanisms [12]. Intrinsically, various ion channels regulate depolarization and repolarization of each individual myocyte. Interestingly, caveolins and caveolae have been associated with many of these ion channels as well as many G proteins that are known to interact with ion channels [4]. Mutations in Cav-3 can lead to congenital long QT syndrome by affecting sodium ion channel regulation [59]. Furthermore, recent studies show that Cav-3 and caveolae are essential for stretch-dependent conduction slowing [40]. Finally, Cav-3 can form macromolecular complexes with one of the major subunits within the cardiac pacemaker channels affecting cardiac conduction [5, 66]. These previous findings and our novel data suggest a critical role for Cav-3 in regulating cardiac conduction and chronotropy.

We show that $K_v1.4$ and $K_v4.3$ channels protein expression levels are significantly increased in Cav-3 OE mice. K_v channels via effects on I_{to} currents are essential to cardiac repolarization. Indeed, when the channel protein expression differences measured in Cav-3 OE mice were used to scale whole-cell ion channel conductances in a mouse ventricular myocyte mode, the APD was shortened. APD_{90} and QTc are closely related [68], and the reduction in APD_{90} from the model (12% at 6 Hz pacing) was similar to the reduction in QTc measured with telemetry (13%). These results suggest that the increase in K_v channel expression is sufficient to explain the QTc decrease in Cav-3 OE mice. Although a severely shortened QT interval has been associated with congenital heart disorders that may cause cardiomyopathy and arrhythmias [44], our mice do not exhibit any characteristics of cardiomyopathy even at old age (unpublished data) and have no increase in mortality when compared to littermate control mice. In contrast, Cav-3 OE mice have been shown to be resistant to myocardial ischemia and demonstrate increased survival in response to chronic pressure overload hypertrophy [20, 55], with decreased hypertrophic response, suggesting a phenotype of stress adaptation. Many different signaling pathways are involved in cardioprotection [19], Cav-3 may serve as a molecular integrator of these various pathways.

Sinus bradycardia and prolonged PR interval are well documented in the trained athlete and are thought to be secondary to unknown intrinsic factors and modified by increased vagal tone on the sinoatrial pacemaker [27, 31]. Our data suggests that caveolins may be an intrinsic factor involved in the cardiac response to exercise via their multiple interactions with ion channels and other cell signaling molecules. Previous investigations have shown that Cav-3 mRNA is up regulated in trained animal hearts approximately 2-fold [18]. Interestingly, our Cav-3 OE mice have an approximate 2-fold elevation of Cav-3 protein at baseline [55]. Short and long-QT syndromes are both uncommon in trained athletes [43]. However, changes within the QT interval are observed during exercise and recovery and are known as QT hysteresis [42]. This shortening in the QT interval is exaggerated in long-QT syndrome and hysteresis has been suggested as a possible marker of long QT [25]. Interestingly, beta-blockade can normalize this exaggerated response as well as lower cardiac risk seen with long-QT syndrome [26, 34]. Furthermore, early repolarization and not terminal repolarization appears to be the major contributor to these changes [23]. The outward potassium current, I_{to}, activates transiently in the sub-threshold range of membrane potential to initiate rapid repolarization following the action potential and helps to set the plateau membrane potential and subsequently the length of the QT interval and action potential duration [35]. In the heart, I_{to} is formed from the heteromeric assembly of three primary alpha subunits ($K_v1.4$, $K_v4.2$ and $K_v4.3$), which are differentially expressed and associated with K_v channel interacting proteins (KChIPs) or the β subunits. The $K_v4.2$ and $K_v4.3$ α subunits contribute to the rapidly recovering ($I_{to,f}$), whereas $K_v1.4$ α subunits contributes to the slowly recovering ($I_{to,s}$) components in the ventricular myocytes [36, 39]. The $K_v4.2$ and $K_v4.3$ channels are shown to partition into caveolae by interacting with the A-kinase anchoring protein, AKAP100, and Cav-3 to form a macromolecular signaling complex [1]. These findings correlate with our results where $K_v1.4$ and $K_v4.3$ channels are overexpressed resulting in faster cardiac repolarization and possibly minimizing exaggerated QT hysteresis.

Cav-3 has also been implicated in voltage-gated sodium channel function. Cav-3 has been shown to co-immunoprecipitate with $Na_v1.5$ [59, 61, 65] (the α-subunit responsible for the inward sodium current resulting in phase 0 of the action potential). Disruption of this channel has been implicated in long QT syndrome type 3 [48, 60, 61] and Brugada Syndrome [45, 49, 50]. Most recently, *in vitro*, co-expression of mutant Cav-3 and $Na_v1.5$ resulted in prolonged action potential duration leading to a long QT type 9 like phenotype [13]. Our results further support the relationship between Cav-3 and $Na_v1.5$ as $Na_v1.5$ is significantly increased in Cav-3 OE mice. However, the effect of increased $Na_v1.5$ expression on the phenotype is uncertain. The action potential model did not support a role for $Na_v1.5$ in the observed QTc decrease. This is consistent with the lack of APD or QTc changes in cardiac specific SCN5A overexpressing mice [67]. The increased $Na_v1.5$ expression may provide a compensatory effect to offset the I_{to} mediated decrease in CaT amplitude predicted by the computational model.

Previous studies have suggested a key role of Cx43 in electrical coupling and action potential propagation [17, 24]. We show that Cx43, a vital component in gap junction formation is increased in Cav-3 OE hearts. An interaction between caveolins and Cx43 has been described [64]. A specific role for Cav-3 in S-nitrosylation of Cx43 in cardiac mitochondria has been suggested [15, 51, 54]. Others have shown that reduction of Cx43 and $Na_v1.5$ results in polymorphic ventricular arrhythmias in cardiac hypertrophy [16]. Interestingly, Cav-3 overexpression has been shown to protect against cardiac hypertrophic remodeling [20, 30].

Extrinsically cardiac conduction is modified via parasympathetic and sympathetic innervation [12]. Standard pharmacological agents were used to investigate the effects of potential extrinsic factors on cardiac conduction in Cav-3 OE mice since caveolae and Cav-3 contain and interact respectively with many of these signaling molecules including GPCRs, G proteins, and adenylyl cyclases [38]. Interestingly, recovery from sympathetic stimulation with dobutamine was faster in Cav-3 OE mice and recovery from sympathetic blockade with propranolol was slower in Cav-3OE mice. Parasympathetic blockade with atropine produced a significant decreased heart rate with a faster recovery in Cav-3 OE mice. Caveolins have been implicated in endocytosis [47] and perhaps Cav-3 OE promotes more efficient clearing of bound receptors that is altered in the presence of an antagonist. In addition, the chronotropic responses to adrenergic agonists were equivocal. These data suggest that Cav-3 overexpression likely does not alter extrinsic mechanisms involved in cardiac conduction, but may improve efficiency and recovery of the cell membrane potential.

The current manuscript has potential limitations. Our data extrapolate ion channel expression to physiological changes and potential computational models. Patch clamp experiments to confirm these data are currently being performed by the laboratory. Similarly, data regarding Cav-3 KO animals that would support our conclusion are currently being performed as well. In addition, the pharmacological experiments were performed with IP injections rather than IV. It is possible that IV administration could result in altered pharmacological responses compared to those we report in this manuscript.

In conclusion, our data suggest that cardiac specific overexpression of Cav-3 results in alterations in baseline cardiac conduction, heart rate, and expression levels of certain cardiac ion channels. Although further investigations are necessary to elucidate the full physiological and clinical implications of Cav-3 overexpression on heart rate control, our novel data support a critical role for Cav-3 in cardiac conduction. The changes observed in baseline cardiac conduction and ion channel expression in our study may provide further mechanistic insight into the phenotype of ischemic tolerance and resistance to pressure overload induced stress that have been observed previously in Cav3- OE mice.

Acknowledgements

We would like to acknowledge the technical assistance of Michael Migita in the performance of the study.

Grants

The work was supported by Veteran Affairs Merit Awards from the Department of Veterans Affairs BX000783 (D. M. Roth), and BX001963 (H. H. Patel), National Institutes of Health HL105713 (R. C. Balijepalli), HL078878 (R. C. Balijepalli), HL091071 (H. H. Patel), HL107200 (H. H. Patel and D.M. Roth), HL066941 (H. H. Patel and D.M. Roth), HL115933 (H. H. Patel and D.M. Roth), GM103426 (A. D. McCulloch), HL105242 (A. D. McCulloch) and EB014593 (A. D. McCulloch). ADM is a co-founder, equity-holder and scientific advisor to Insilicomed, Inc.. This relationship is managed by a UCSD Conflict of Interest sub-committee. However, there was no involvement of Insilicomed, Inc. in the research described here.

Abbreviations

AKAP100	A-kinase anchoring protein
ANOVA	analysis of variance
APD	action potential duration
bpm	beats per minute
CO_2	carbon dioxide
Cav-3	Caveolin-3
CaT	calcium transients
Cx43	Connexin 43
ECG	electrocardiogram
EDTA	ethylenediaminetetraacetic acid
GAPDH	glyceraldehyde 3-phosphate dehydrogenase
G_{Na}	conductance of fast sodium channel
GPCRs	G-protein coupled receptors
$G_{to,f}$	conductance of fast transient outward potassium current
Hz	hertz
hr	hour

$I_{to,s}$	slow component of transient outward potassium current
kcal	kilocalorie
K_v	voltage gated potassium channel
KChIPs	K_v channel interacting proteins
ml	milliliter
mRNA	messenger Ribonucleic acid
mS	millisiemens
µF	microfarad
Na_v	voltage gated sodium channel
O_2	oxygen
OE	over expression
PAGE	polyacrylamide gel electrophoresis
pH	power of hydrogen
RER	respiratory exchange ratio
SCN5A	sodium channel, voltage gated, type V alpha subunit
SD	standard deviation
SDS	sodium dodecyl sulfate
Tris-HCL	tris-hydrochlorite

References

1. Alday A, Urrutia J, Gallego M, Casis O. alpha1-adrenoceptors regulate only the caveolae-located subpopulation of cardiac K(V)4 channels. Channels (Austin, Tex.). 2010; 4:168–178. doi:10.4161/chan.4.3.11479.
2. Balijepalli RC, Delisle BP, Balijepalli SY, Foell JD, Slind JK, Kamp TJ, January CT. Kv11.1 (ERG1) K+ channels localize in cholesterol and sphingolipid enriched membranes and are modulated by membrane cholesterol. Channels (Austin, Tex.). 2007; 1:263–272. doi:10.4161/chan.4946.
3. Balijepalli RC, Foell JD, Hall DD, Hell JW, Kamp TJ. Localization of cardiac L-type Ca(2+) channels to a caveolar macromolecular signaling complex is required for beta(2)-adrenergic regulation. Proc Natl Acad Sci U S A. 2006; 103:7500–7505. doi:10.1073/pnas.0503465103. [PubMed: 16648270]
4. Balijepalli RC, Kamp TJ. Caveolae, ion channels and cardiac arrhythmias. Prog Biophys Mol Biol. 2008; 98:149–160. doi:10.1016/j.pbiomolbio.2009.01.012. [PubMed: 19351512]
5. Barbuti A, Gravante B, Riolfo M, Milanesi R, Terragni B, DiFrancesco D. Localization of pacemaker channels in lipid rafts regulates channel kinetics. Circ Res. 2004; 94:1325–1331. doi:10.1161/01.RES.0000127621.54132.AE. [PubMed: 15073040]
6. Benoist D, Stones R, Drinkhill M, Bernus O, White E. Arrhythmogenic substrate in hearts of rats with monocrotaline-induced pulmonary hypertension and right ventricular hypertrophy. Am J

Physiol Heart Circ Physiol. 2011; 300:H2230–2237. doi:10.1152/ajpheart.01226.2010. [PubMed: 21398591]

7. Bossuyt J, Taylor BE, James-Kracke M, Hale CC. The cardiac sodium-calcium exchanger associates with caveolin-3. Ann N Y Acad Sci. 2002; 976:197–204. doi:10.1111/j.1749-6632.2002.tb04741.x. [PubMed: 12502561]
8. Bossuyt J, Taylor BE, James-Kracke M, Hale CC. Evidence for cardiac sodium-calcium exchanger association with caveolin-3. FEBS Lett. 2002; 511:113–117. doi:10.1016/S0014-5793(01)03323-3. [PubMed: 11821059]
9. Chandler NJ, Greener ID, Tellez JO, Inada S, Musa H, Molenaar P, Difrancesco D, Baruscotti M, Longhi R, Anderson RH, Billeter R, Sharma V, Sigg DC, Boyett MR, Dobrzynski H. Molecular architecture of the human sinus node: insights into the function of the cardiac pacemaker. Circulation. 2009; 119:1562–1575. doi:10.1161/circulationaha.108.804369. [PubMed: 19289639]
10. Cheng J, Valdivia CR, Vaidyanathan R, Balijepalli RC, Ackerman MJ, Makielski JC. Caveolin-3 suppresses late sodium current by inhibiting nNOS-dependent S-nitrosylation of SCN5A. J Mol Cell Cardiol. 2013; 61:102–110. doi:10.1016/j.yjmcc.2013.03.013. [PubMed: 23541953]
11. Cohen AW, Hnasko R, Schubert W, Lisanti MP. Role of caveolae and caveolins in health and disease. Physiol Rev. 2004; 84:1341–1379. doi:10.1152/physrev.00046.2003 84/4/1341 [pii]. [PubMed: 15383654]
12. Conrath CE, Opthof T. Ventricular repolarization: an overview of (patho)physiology, sympathetic effects and genetic aspects. Prog Biophys Mol Biol. 2006; 92:269–307. doi:10.1016/j.pbiomolbio.2005.05.009. [PubMed: 16023179]
13. Cronk LB, Ye B, Kaku T, Tester DJ, Vatta M, Makielski JC, Ackerman MJ. Novel mechanism for sudden infant death syndrome: persistent late sodium current secondary to mutations in caveolin-3. Heart Rhythm. 2007; 4:161–166. doi:10.1016/j.hrthm.2006.11.030. [PubMed: 17275750]
14. Dhein S, Seidel T, Salameh A, Jozwiak J, Hagen A, Kostelka M, Hindricks G, Mohr FW. Remodeling of cardiac passive electrical properties and susceptibility to ventricular and atrial arrhythmias. Front Physiol. 2014; 5:424. doi:10.3389/fphys.2014.00424. [PubMed: 25404918]
15. Ferdinandy P, Hausenloy DJ, Heusch G, Baxter GF, Schulz R. Interaction of risk factors, comorbidities, and comedications with ischemia/reperfusion injury and cardioprotection by preconditioning, postconditioning, and remote conditioning. Pharmacol Rev. 2014; 66:1142–1174. doi:10.1124/pr.113.008300. [PubMed: 25261534]
16. Fontes MS, Raaijmakers AJ, van Doorn T, Kok B, Nieuwenhuis S, van der Nagel R, Vos MA, de Boer TP, van Rijen HV, Bierhuizen MF. Changes in Cx43 and NaV1.5 expression precede the occurrence of substantial fibrosis in calcineurin-induced murine cardiac hypertrophy. PloS one. 2014; 9:e87226. doi:10.1371/journal.pone.0087226. [PubMed: 24498049]
17. Fontes MS, van Veen TA, de Bakker JM, van Rijen HV. Functional consequences of abnormal Cx43 expression in the heart. Biochim Biophys Acta. 2012; 1818:2020–2029. doi:10.1016/j.bbamem.2011.07.039. [PubMed: 21839722]
18. Giusti B, Marini M, Rossi L, Lapini I, Magi A, Capalbo A, Lapalombella R, di Tullio S, Samaja M, Esposito F, Margonato V, Boddi M, Abbate R, Veicsteinas A. Gene expression profile of rat left ventricles reveals persisting changes following chronic mild exercise protocol: implications for cardioprotection. BMC Genomics. 2009; 10:342. doi:10.1186/1471-2164-10-342. [PubMed: 19643001]
19. Heusch G. Molecular basis of cardioprotection: signal transduction in ischemic pre-, post-, and remote conditioning. Circ Res. 2015; 116:674–699. doi:10.1161/circresaha.116.305348. [PubMed: 25677517]
20. Horikawa YT, Panneerselvam M, Kawaraguchi Y, Tsutsumi YM, Ali SS, Balijepalli RC, Murray F, Head BP, Niesman IR, Rieg T, Vallon V, Insel PA, Patel HH, Roth DM. Cardiac-specific overexpression of caveolin-3 attenuates cardiac hypertrophy and increases natriuretic peptide expression and signaling. J Am Coll Cardiol. 2011; 57:2273–2283. doi:10.1016/j.jacc.2010.12.032. [PubMed: 21616289]
21. Horikawa YT, Patel HH, Tsutsumi YM, Jennings MM, Kidd MW, Hagiwara Y, Ishikawa Y, Insel PA, Roth DM. Caveolin-3 expression and caveolae are required for isoflurane-induced cardiac protection from hypoxia and ischemia/reperfusion injury. J Mol Cell Cardiol. 2008; 44:123–130. doi:10.1016/j.yjmcc.2007.10.003. [PubMed: 18054955]

22. Horikawa YT, Tsutsumi YM, Patel HH, Roth DM. Signaling epicenters: the role of caveolae and caveolins in volatile anesthetic induced cardiac protection. Curr Pharm Des. 2014; 20:5681–5689. doi:10.2174/1381612820666140204111236. [PubMed: 24502576]

23. Kannankeril PJ, Harris PA, Norris KJ, Warsy I, Smith PD, Roden DM. Rate-independent QT shortening during exercise in healthy subjects: terminal repolarization does not shorten with exercise. J Cardiovasc Electrophysiol. 2008; 19:1284–1288. doi:10.1111/j.1540-8167.2008.01266.x. [PubMed: 18665873]

24. Kleber AG, Rudy Y. Basic mechanisms of cardiac impulse propagation and associated arrhythmias. Physiol Rev. 2004; 84:431–488. doi:10.1152/physrev.00025.2003. [PubMed: 15044680]

25. Krahn AD, Klein GJ, Yee R. Hysteresis of the RT interval with exercise: a new marker for the long-QT syndrome? Circulation. 1997; 96:1551–1556. doi:10.1161/01.CIR.96.5.1551. [PubMed: 9315546]

26. Krahn AD, Yee R, Chauhan V, Skanes AC, Wang J, Hegele RA, Klein GJ. Beta blockers normalize QT hysteresis in long QT syndrome. American heart journal. 2002; 143:528–534. doi:10.1067/mhj.2002.120408. [PubMed: 11868061]

27. Lampert R. Evaluation and management of arrhythmia in the athletic patient. Progress in cardiovascular diseases. 2012; 54:423–431. doi:10.1016/j.pcad.2012.01.002. [PubMed: 22386293]

28. Lohn M, Furstenau M, Sagach V, Elger M, Schulze W, Luft FC, Haller H, Gollasch M. Ignition of calcium sparks in arterial and cardiac muscle through caveolae. Circ Res. 2000; 87:1034–1039. doi:10.1161/01.RES.87.11.1034. [PubMed: 11090549]

29. Markandeya YS, Fahey JM, Pluteanu F, Cribbs LL, Balijepalli RC. Caveolin-3 regulates protein kinase A modulation of the Ca(V)3.2 (alpha1H) T-type Ca2+ channels. J Biol Chem. 2011; 286:2433–2444. doi:10.1074/jbc.M110.182550. [PubMed: 21084288]

30. Markandeya YS, Phelan LJ, Woon MT, Keefe AM, Reynolds CR, August BK, Hacker TA, Roth DM, Patel HH, Balijepalli RC. Caveolin-3 Overexpression Attenuates Cardiac Hypertrophy via Inhibition of T-type Ca2+ Current Modulated by Protein Kinase Calpha in Cardiomyocytes. J Biol Chem. 2015; 290:22085–22100. doi:10.1074/jbc.M115.674945. [PubMed: 26170457]

31. Maron BJ, Pelliccia A. The heart of trained athletes: cardiac remodeling and the risks of sports, including sudden death. Circulation. 2006; 114:1633–1644. doi:10.1161/CIRCULATIONAHA.106.613562. [PubMed: 17030703]

32. Mitchell GF, Jeron A, Koren G. Measurement of heart rate and Q-T interval in the conscious mouse. Am J Physiol. 1998; 274:H747–751. [PubMed: 9530184]

33. Morotti S, Edwards AG, McCulloch AD, Bers DM, Grandi E. A novel computational model of mouse myocyte electrophysiology to assess the synergy between Na+ loading and CaMKII. J Physiol. 2014; 592:1181–1197. doi:10.1113/jphysiol.2013.266676. [PubMed: 24421356]

34. Moss AJ, Zareba W, Hall WJ, Schwartz PJ, Crampton RS, Benhorin J, Vincent GM, Locati EH, Priori SG, Napolitano C, Medina A, Zhang L, Robinson JL, Timothy K, Towbin JA, Andrews ML. Effectiveness and limitations of beta-blocker therapy in congenital long-QT syndrome. Circulation. 2000; 101:616–623. doi:10.1161/01.CIR.101.6.616. [PubMed: 10673253]

35. Nerbonne JM, Kass RS. Molecular physiology of cardiac repolarization. Physiol Rev. 2005; 85:1205–1253. doi:10.1152/physrev.00002.2005. [PubMed: 16183911]

36. Niwa N, Nerbonne JM. Molecular determinants of cardiac transient outward potassium current (I(to)) expression and regulation. J Mol Cell Cardiol. 2010; 48:12–25. doi:10.1016/j.yjmcc.2009.07.013. [PubMed: 19619557]

37. Palade G. Fine structure of blood capillaries. J of Appl Phys. 1953; 24:1424–1436.

38. Patel HH, Murray F, Insel PA. Caveolae as organizers of pharmacologically relevant signal transduction molecules. Annu Rev Pharmacol Toxicol. 2008; 48:359–391. doi:10.1146/annurev.pharmtox.48.121506.124841. [PubMed: 17914930]

39. Patel SP, Campbell DL. Transient outward potassium current, 'Ito', phenotypes in the mammalian left ventricle: underlying molecular, cellular and biophysical mechanisms. J Physiol. 2005; 569:7–39. doi:10.1113/jphysiol.2005.086223. [PubMed: 15831535]

40. Pfeiffer ER, Wright AT, Edwards AG, Stowe JC, McNall K, Tan J, Niesman I, Patel HH, Roth DM, Omens JH, McCulloch AD. Caveolae in ventricular myocytes are required for stretch-dependent

conduction slowing. J Mol Cell Cardiol. 2014; 76:265–274. doi:10.1016/j.yjmcc.2014.09.014. [PubMed: 25257915]

41. Razani B, Woodman SE, Lisanti MP. Caveolae: from cell biology to animal physiology. Pharmacol Rev. 2002; 54:431–467. doi:10.1124/pr.54.3.431. [PubMed: 12223531]
42. Sarma JS, Venkataraman SK, Samant DR, Gadgil U. Hysteresis in the human RRQT relationship during exercise and recovery. Pacing and clinical electrophysiology : PACE. 1987; 10:485–491. [PubMed: 2439996]
43. Scharhag J, Lollgen H, Kindermann W. Competitive sports and the heart: benefit or risk? Deutsches Arzteblatt international. 2013; 110:14–23. e11–12. quiz 24, doi:10.3238/arztebl.2013.0014. [PubMed: 23450998]
44. Schimpf R, Borggrefe M, Wolpert C. Clinical and molecular genetics of the short QT syndrome. Curr Opin Cardiol. 2008; 23:192–198. doi:10.1097/HCO.0b013e3282fbf756. [PubMed: 18382206]
45. Schulze-Bahr E, Eckardt L, Breithardt G, Seidl K, Wichter T, Wolpert C, Borggrefe M, Haverkamp W. Sodium channel gene (SCN5A) mutations in 44 index patients with Brugada syndrome: different incidences in familial and sporadic disease. Human mutation. 2003; 21:651–652. doi:10.1002/humu.9144.
46. See Hoe LE, Schilling JM, Tarbit E, Kiessling CJ, Busija AR, Niesman IR, Du Toit E, Ashton KJ, Roth DM, Headrick JP, Patel HH, Peart JN. Sarcolemmal cholesterol and caveolin-3 dependence of cardiac function, ischemic tolerance, and opioidergic cardioprotection. Am J Physiol Heart Circ Physiol. 2014; 307:H895–903. doi:10.1152/ajpheart.00081.2014. [PubMed: 25063791]
47. Shvets E, Ludwig A, Nichols BJ. News from the caves: update on the structure and function of caveolae. Curr Opin Cell Biol. 2014; 29:99–106. doi:10.1016/j.ceb.2014.04.011. [PubMed: 24908346]
48. Shy D, Gillet L, Abriel H. Cardiac sodium channel NaV1.5 distribution in myocytes via interacting proteins: the multiple pool model. Biochim Biophys Acta. 2013; 1833:886–894. doi:10.1016/j.bbamcr.2012.10.026. [PubMed: 23123192]
49. Smits JP, Eckardt L, Probst V, Bezzina CR, Schott JJ, Remme CA, Haverkamp W, Breithardt G, Escande D, Schulze-Bahr E, LeMarec H, Wilde AA. Genotypephenotype relationship in Brugada syndrome: electrocardiographic features differentiate SCN5A-related patients from non-SCN5A-related patients. J Am Coll Cardiol. 2002; 40:350–356. doi:10.1016/S0735-1097(02)01962-9. [PubMed: 12106943]
50. Smits JP, Wilde AA. Brugada syndrome: in search of a genotype-phenotype relationship. Herzschrittmachertherapie & Elektrophysiologie. 2002; 13:142–148. doi:10.1007/s00399-002-0350-9. [PubMed: 24535448]
51. Soetkamp D, Nguyen TT, Menazza S, Hirschhauser C, Hendgen-Cotta UB, Rassaf T, Schluter KD, Boengler K, Murphy E, Schulz R. S-nitrosation of mitochondrial connexin 43 regulates mitochondrial function. Basic Res Cardiol. 2014; 109:433. doi:10.1007/s00395-014-0433-x. [PubMed: 25115184]
52. Song KS, Scherer PE, Tang Z, Okamoto T, Li S, Chafel M, Chu C, Kohtz DS, Lisanti MP. Expression of caveolin-3 in skeletal, cardiac, and smooth muscle cells. Caveolin-3 is a component of the sarcolemma and co-fractionates with dystrophin and dystrophin-associated glycoproteins. J Biol Chem. 1996; 271:15160–15165. [PubMed: 8663016]
53. Steinberg SF, Brunton LL. Compartmentation of G protein-coupled signaling pathways in cardiac myocytes. Annu Rev Pharmacol Toxicol. 2001; 41:751–773. doi:10.1146/annurev.pharmtox.41.1.751. [PubMed: 11264475]
54. Sun J, Nguyen T, Aponte AM, Menazza S, Kohr MJ, Roth DM, Patel HH, Murphy E, Steenbergen C. Ischaemic preconditioning preferentially increases protein S-nitrosylation in subsarcolemmal mitochondria. Cardiovasc Res. 2015; 106:227–236. doi:10.1093/cvr/cvv044. [PubMed: 25694588]
55. Tsutsumi YM, Horikawa YT, Jennings MM, Kidd MW, Niesman IR, Yokoyama U, Head BP, Hagiwara Y, Ishikawa Y, Miyanohara A, Patel PM, Insel PA, Patel HH, Roth DM. Cardiac-specific overexpression of caveolin-3 induces endogenous cardiac protection by mimicking ischemic preconditioning. Circulation. 2008; 118:1979–1988. doi:CIRCULATIONAHA.108.788331 [pii] 10.1161/CIRCULATIONAHA.108.788331. [PubMed: 18936328]

56. Tsutsumi YM, Horikawa YT, Jennings MM, Kidd MW, Niesman IR, Yokoyama U, Head BP, Hagiwara Y, Ishikawa Y, Miyanohara A, Patel PM, Insel PA, Patel HH, Roth DM. Cardiac-specific overexpression of caveolin-3 induces endogenous cardiac protection by mimicking ischemic preconditioning. Circulation. 2008; 118:1979–1988. doi:10.1161/CIRCULATIONAHA.108.788331. [PubMed: 18936328]
57. Tsutsumi YM, Tsutsumi R, Horikawa YT, Sakai Y, Hamaguchi E, Ishikawa Y, Yokoyama U, Kasai A, Kambe N, Tanaka K. Geranylgeranylacetone protects the heart via caveolae and caveolin-3. Life Sci. 2014; 101:43–48. doi:10.1016/j.lfs.2014.02.019. [PubMed: 24582814]
58. Tsutsumi YM, Tsutsumi R, Horikawa YT, Sakai Y, Hamaguchi E, Kitahata H, Kasai A, Kambe N, Tanaka K. Geranylgeranylacetone and volatile anesthetic-induced cardiac protection synergism is dependent on caveolae and caveolin-3. Journal of anesthesia. 2014; 28:733–739. doi:10.1007/s00540-014-1816-8. [PubMed: 24633659]
59. Vatta M, Ackerman MJ, Ye B, Makielski JC, Ughanze EE, Taylor EW, Tester DJ, Balijepalli RC, Foell JD, Li Z, Kamp TJ, Towbin JA. Mutant caveolin-3 induces persistent late sodium current and is associated with long-QT syndrome. Circulation. 2006; 114:2104–2112. doi:10.1161/CIRCULATIONAHA.106.635268. [PubMed: 17060380]
60. Wang Q, Shen J, Splawski I, Atkinson D, Li Z, Robinson JL, Moss AJ, Towbin JA, Keating MT. SCN5A mutations associated with an inherited cardiac arrhythmia, long QT syndrome. Cell. 1995; 80:805–811. [PubMed: 7889574]
61. Willis BC, Ponce-Balbuena D, Jalife J. Protein assemblies of sodium and inward rectifier potassium channels control cardiac excitability and arrhythmogenesis. Am J Physiol Heart Circ Physiol. 2015; 308:H1463–1473. doi:10.1152/ajpheart.00176.2015. [PubMed: 25862830]
62. Xu H, Guo W, Nerbonne JM. Four kinetically distinct depolarization-activated K+ currents in adult mouse ventricular myocytes. J Gen Physiol. 1999; 113:661–678. doi:10.1085/jgp.113.5.661. [PubMed: 10228181]
63. Yamada E. The fine structure of the gall bladder epithelium of the mouse. J Biophys Biochem Cytol. 1955; 1:445–458. [PubMed: 13263332]
64. Yang KC, Rutledge CA, Mao M, Bakhshi FR, Xie A, Liu H, Bonini MG, Patel HH, Minshall RD, Dudley SC Jr. Caveolin-1 modulates cardiac gap junction homeostasis and arrhythmogenecity by regulating cSrc tyrosine kinase. Circulation. Arrhythmia and electrophysiology. 2014; 7:701–710. doi:10.1161/CIRCEP.113.001394. [PubMed: 25017399]
65. Yarbrough TL, Lu T, Lee HC, Shibata EF. Localization of cardiac sodium channels in caveolin-rich membrane domains: regulation of sodium current amplitude. Circ Res. 2002; 90:443–449. doi:10.1161/hh0402.105177. [PubMed: 11884374]
66. Ye B, Balijepalli RC, Foell JD, Kroboth S, Ye Q, Luo YH, Shi NQ. Caveolin-3 associates with and affects the function of hyperpolarization-activated cyclic nucleotide-gated channel 4. Biochemistry. 2008; 47:12312–12318. doi:10.1021/bi8009295. [PubMed: 19238754]
67. Zhang T, Yong SL, Tian XL, Wang QK. Cardiac-specific overexpression of SCN5A gene leads to shorter P wave duration and PR interval in transgenic mice. Biochem Biophys Res Commun. 2007; 355:444–450. doi:10.1016/j.bbrc.2007.01.170. [PubMed: 17300750]
68. Zhang Y, Wu J, King JH, Huang CL, Fraser JA. Measurement and interpretation of electrocardiographic QT intervals in murine hearts. Am J Physiol Heart Circ Physiol. 2014; 306:H1553–1557. doi:10.1152/ajpheart.00459.2013. [PubMed: 24705556]

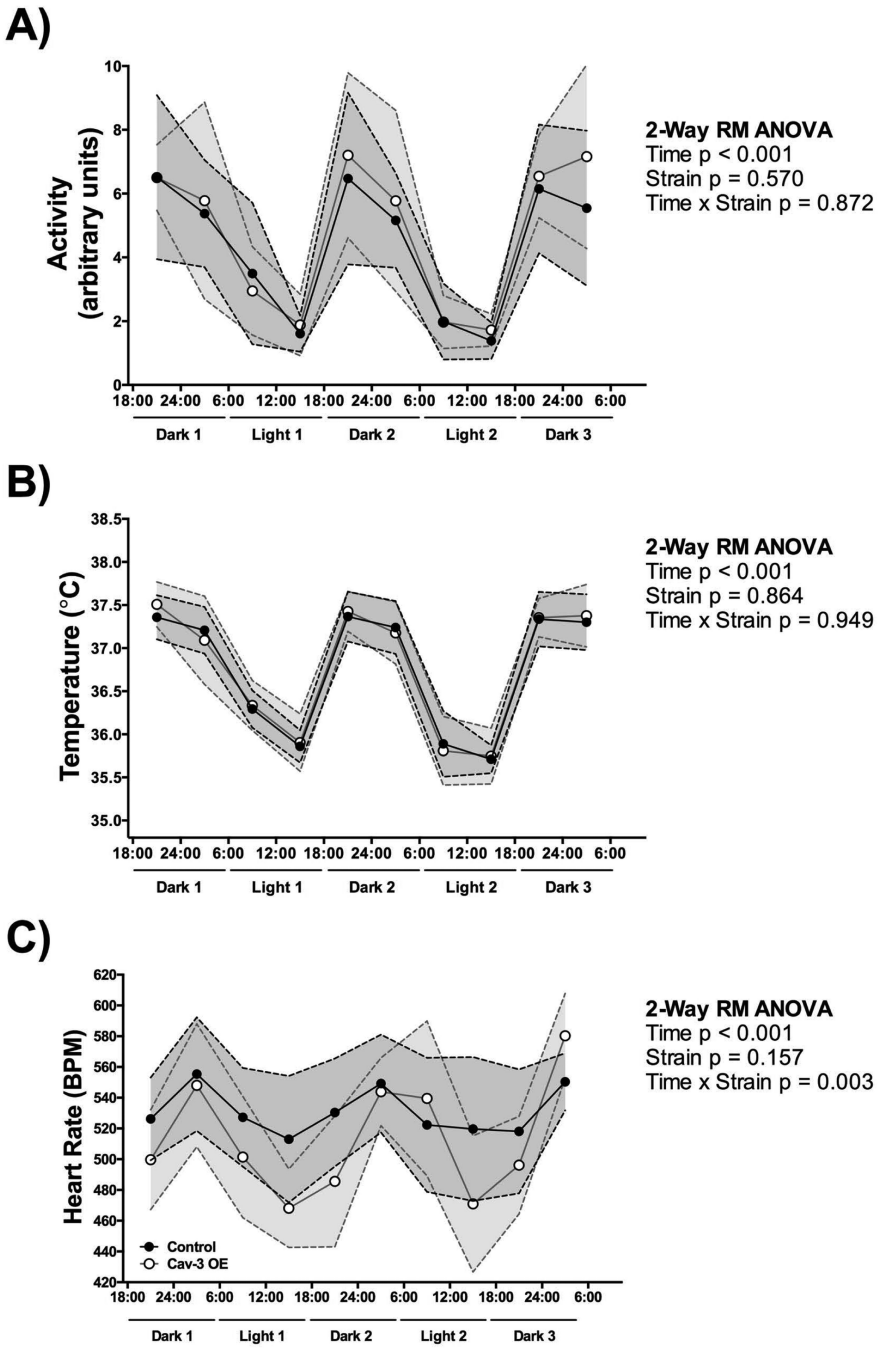

Figure 1.

Cav-3 OE mice have **(A)** similar baseline activity and **(B)** body temperature fluctuation, and **(C)** a significantly higher heart rate fluctuation with overall lower heart rates compared to control mice. *P* is assumed significant when < 0.05; Data are presented as *Mean* ± *SD*; *N* = 7 - 8/group.

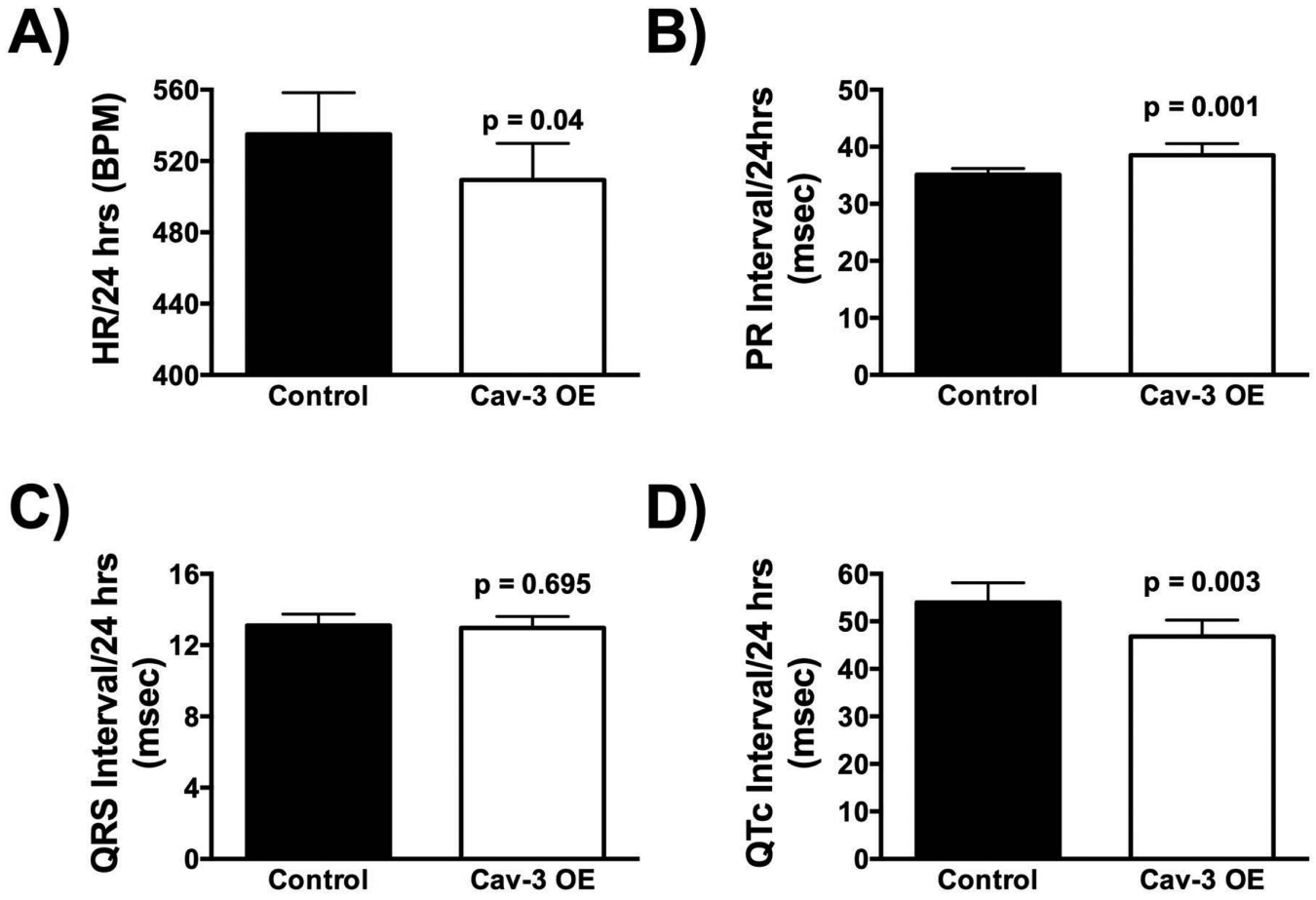

Figure 2.

Cav-3 OE mice show **(A)** lower 24hr heart rates, **(B)** prolonged PR intervals, **(C)** no significant difference in overall QRS complex length, and **(D)** shortened QT intervals. *P* is assumed significant when < 0.05; Data are presented as *Mean* ± *SD*; *N* = 7 - 8/group.

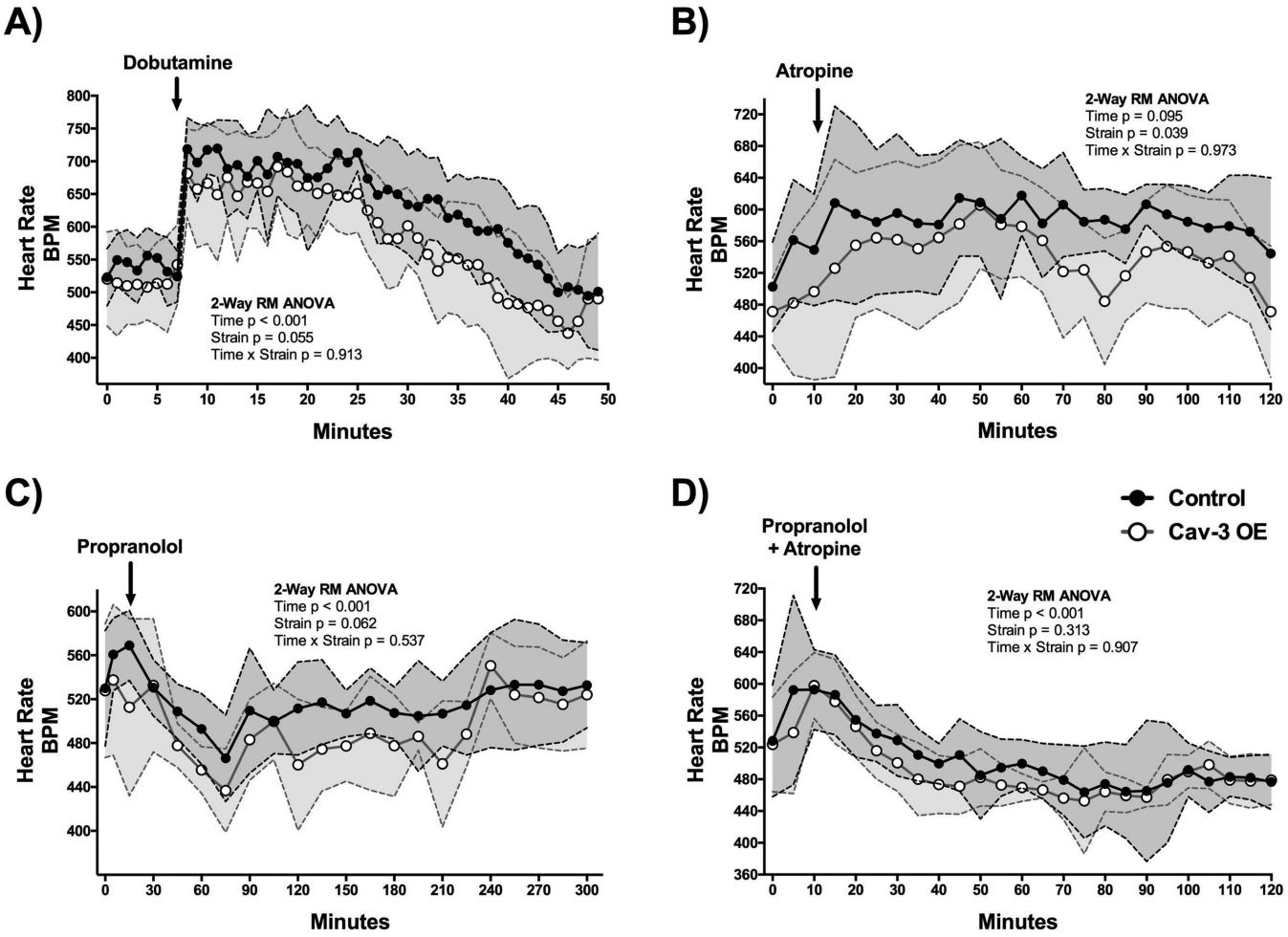

Figure 3.

Cav-3 OE mice show a trending ($p < 0.1$) difference to **(A)** β_1-adrenergic stimulation with dobutamine, **(B)** a significant lower response to muscarinic inhibition with atropine, and **(C)** a trending decreased response to non-specific β-adrenergic blockade with propranolol. **(D)** No significant difference between groups was observed upon parallel administration of propranolol and atropine. *P* is assumed significant when < 0.05; Data are presented as *Mean* ± *SD*; *N* = 7 - 8/group.

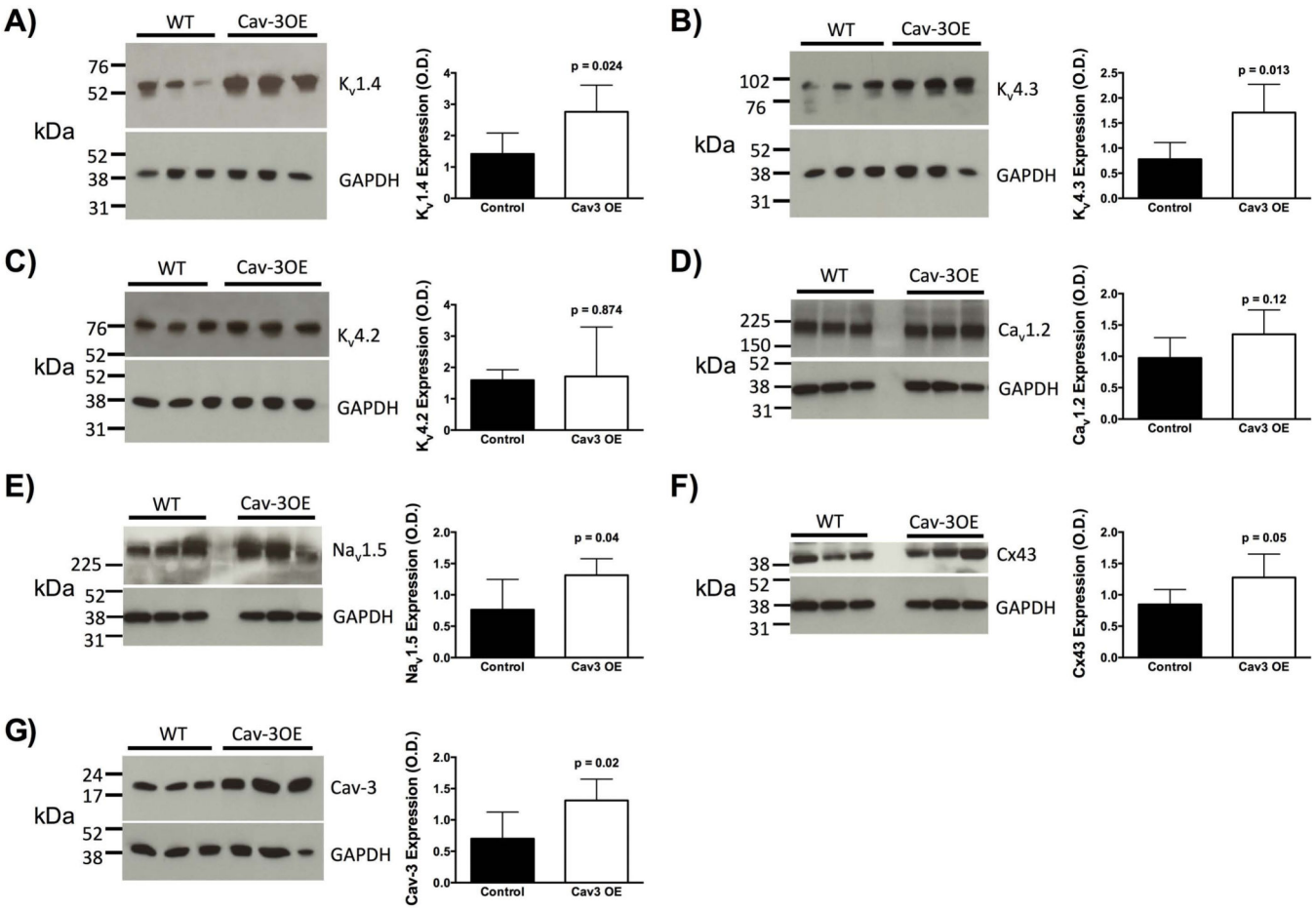

Figure 4.

Left ventricular tissue from Cav-3 OE mice showed increased protein expression of $K_V1.4$ **(A)**, and $K_V4.3$ **(B)**, no change in $K_V4.2$ **(C)** and $Ca_V1.2$ **(D)**, but increased protein levels of in $Na_V1.5$ **(E)** and Cx43 **(F)**. Elevated Cav-3 protein expression was confirmed in Cav-3 OE hearts **(G)**. *P* is assumed significant when < 0.05; Data are presented as *Mean* ± *SD*; *N* = 5 - 7/group.

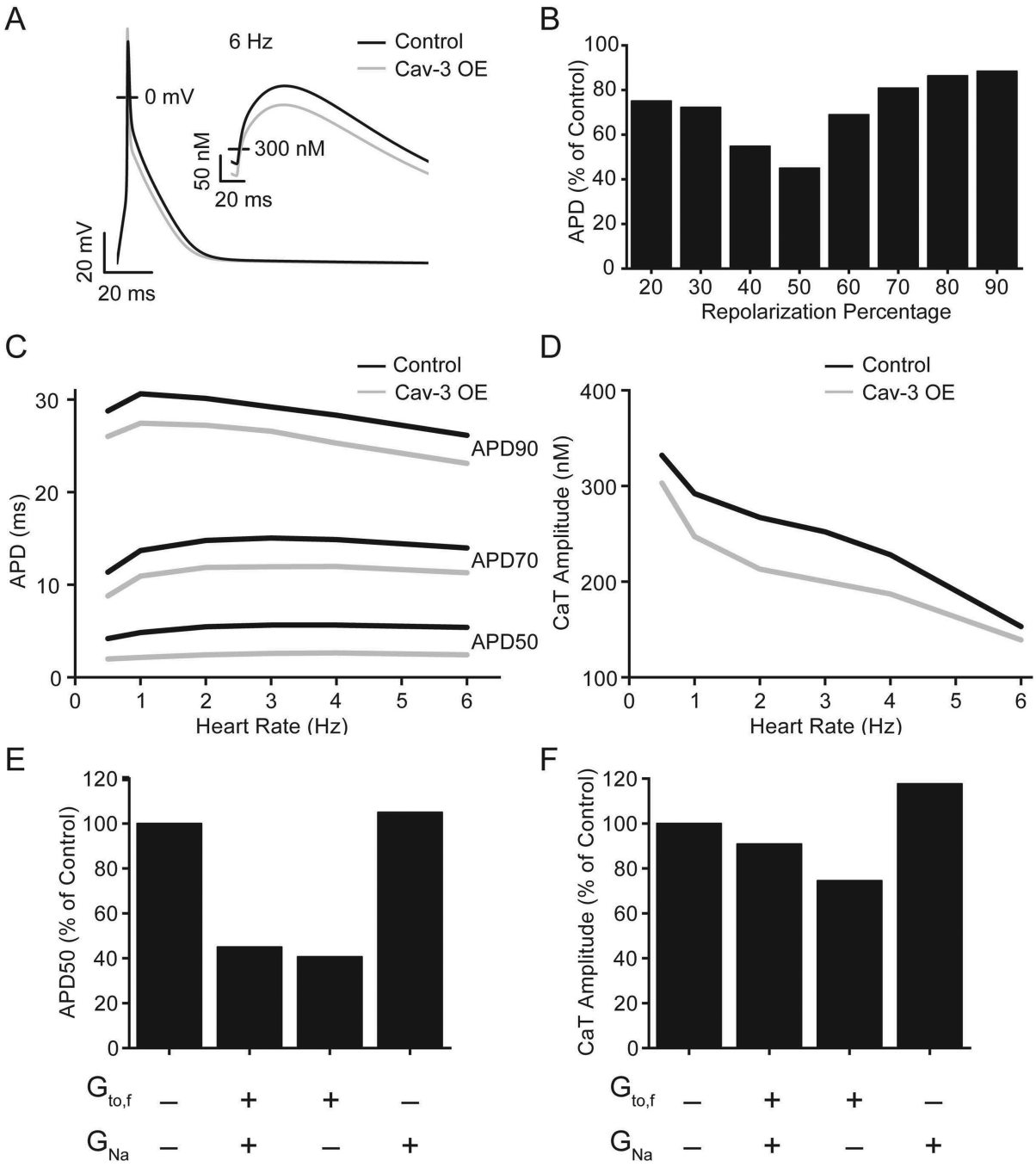

Figure 5.

Computational modeling results. **(A)** Action potential and intracellular Ca^{2+} (inset) from simulated 6 Hz pacing for control (black line) and Cav-3 OE (grey line) model parameters. **(B)** APD was decreased in the Cav-3 OE model compared to control. **(C)** This decrease was consistent across a range of pacing rates. **(D)** Intracellular calcium transient amplitude was slightly decreased in the Cav-3 OE model with the effect diminishing near physiological

rates. **(E)** The increase in $G_{to,f}$ was responsible for the decrease in APD. **(F)** Increasing $G_{to,f}$ and G_{Na} had opposing effects on the CaT amplitude when applied individually.

Table 1

CLAMS metabolic cage results

Time (light and dark cycle) had a significant effect on all parameters. No significant effect of strain or interaction was found for other parameters measured in metabolic profiling cages.

		Control	Cau-3 OE	Statistics		F (DFn, DFd)	P value
Weight (grams)	**Before**	25.94 ± 1.77	25.82 ± 2.49	**2-Way RM ANOVA**	**Time**	F (1, 10) = 12.65	P = 0.005
	After	24.52 ± 1.53	25.12 ± 2.63		**Strain**	F (1, 10) = 0.04	P = 0.845
					Interaction	F (1, 10) = 1.482	P = 0.252
						t (df)	
	Change	−1.42 ± 1.12	−0.70 ± 0.93	**t test**	**unpaired**	t (10) = 1.217	P = 0.252
VO_2 (ml/kg/hr)	**Dark 1**	4488.15 ± 219.92	4402.29 ± 255.72	**2-Way RM ANOVA**	**Time**	F (4, 40) = 63.89	P < 0.001
	Light 1	3965.26 ± 270.28	3894.60 ± 267.46		**Strain**	F (1, 10) = 0.086	P = 0.776
	Dark 2	4691.70 ± 229.34	4643.84 ± 361.87		**Interaction**	F (4, 40) = 0.499	P = 0.737
	Light 2	3979.32 ± 179.73	3905.65 ± 249.86				
	Dark 3	4495.64 ± 365.01	4558.41 ± 393.24				
VCO_2 (ml/kg/hr)	**Dark 1**	4057.02 ± 196.67	3978.93 ± 345.03	**2-Way RM ANOVA**	**Time**	F (4, 40) = 47.79	P < 0.001
	Light 1	3440.59 ± 263.67	3476.22 ± 253.98		**Strain**	F (1, 10) < 0.001	P = 0.998
	Dark 2	4289.97 ± 185.37	4278.28 ± 345.75		**Interaction**	F (4, 40) = 0.166	P = 0.954
	Light 2	3322.22 ± 142.58	3365.32 ± 205.61				
	Dark 3	4076.90 ± 468.88	4085.79 ± 442.01				
RER	**Dark 1**	0.90 ± 0.02	0.90 ± 0.04	**2-Way RM ANOVA**	**Time**	F (4, 40) = 9.095	P < 0.001
	Light 1	0.87 ± 0.02	0.89 ± 0.02		**Strain**	F (1, 10) = 1.517	P = 0.246
	Dark 2	0.91 ± 0.02	0.92 ± 0.02		**Interaction**	F (4, 40) = 0.732	P = 0.576
	Light 2	0.83 ± 0.04	0.86 ± 0.01				
	Dark 3	0.90 ± 0.05	0.89 ± 0.05				
Heat (kcal/hr)	**Dark 1**	0.57 ± 0.05	0.56 ± 0.04	**2-Way RM ANOVA**	**Time**	F (4, 40) = 70.52	P < 0.001
	Light 1	0.50 ± 0.06	0.49 ± 0.04		**Strain**	F (1, 10) = 0.075	P = 0.789
	Dark 2	0.60 ± 0.05	0.59 ± 0.04		**Interaction**	F (4, 40) = 0.198	P = 0.938
	Light 2	0.50 ± 0.04	0.49 ± 0.03				
	Dark 3	0.58 ± 0.06	0.58 ± 0.04				

		Control	Cau-3 OE	Statistics		F (DFn, DFd)	P value
Feeding, accumulated (grams)	**Dark 1**	2.36 ± 0.82	1.97 ± 0.61	**2-Way RM ANOVA**	**Time**	F (4, 40) = 1471	P < 0.001
	Light 1	5.31 ± 1.66	4.58 ± 0.65		**Strain**	F (1, 10) = 0.991	P = 0.343
	Dark 2	8.05 ± 1.86	7.21 ± 0.77		**Interaction**	F (4, 40) = 0.681	P = 0.609
	Light 2	10.28 ± 1.70	9.54 ± 0.86				
	Dark 3	12.76 ± 1.56	12.08 ± 0.75				
Drinking, accumulated (ml)	**Dark 1**	1.48 ± 0.33	1.66 ± 0.43	**2-Way RM ANOVA**	**Time**	F (4, 40) = 1037	P < 0.001
	Light 1	3.97 ± 0.54	3.98 ± 0.59		**Strain**	F (1, 10) = 0.025	P = 0.878
	Dark 2	6.22 ± 0.68	6.18 ± 0.52		**Interaction**	F (4, 40) = 0.135	P = 0.969
	Light 2	8.39 ± 0.87	8.43 ± 0.63				
	Dark 3	10.57 ± 1.17	10.65 ± 0.76				

Data are Mean ± SD. Significance was assumed when $p < 0.05$. VO2: oxygen consumption; VCO2: carbon dioxide elimination; RER: respiratory exchange ratio